

# **Predicting Radiation-Induced Transient Response in HgCdTe Sensor Arrays**

**Final Report – September 30, 2006**

REAG has been tasked with predicting the on-orbit radiation induced transient response in the JWST focal plane arrays (FPA) in the context of assessing the impact on acquisition of science data. Since this is a problem of general interest, NEPP also contributed to the analysis. Pre-mission knowledge of the transient response will allow mission planners to optimize the observatory design and performance. The dominant on-orbit radiation environment at L2 is GeV-range protons from the galactic cosmic rays (GCR). In addition, there will be protons at the FPA in the range of ten to a few hundred MeV from solar particle events (SPE). However, it is assumed that science data acquisition will not be attempted during solar particle events. The SPE protons are a concern for degradation but not for transients.

It is not feasible to perform ground-based testing with protons in the GeV energy range with the full-up FPA configuration (FPA and surrounding material) of the observatory. Thus, our approach is to use a combination of modeling and testing to develop and calibrate an FPA transient response model. We will then use the FPA model in conjunction with particle transport modeling through the surrounding material to determine the on-orbit local particle environment at the FPA and then the response of the FPA to the local environment.

An extensive series of tests have been performed on representative arrays of the H2RG FPA technology that will be used on JWST. Testing was performed with protons at energies of 30 and 63 MeV and at angles of incidence of 0, 45 and 67 degrees. One of the purposes of the tests was to evaluate the FPA response model, designated REACT (Radiation Environment Array Charge Transport). REACT is an engineering model that is based on our best understanding of the physics involved but is geared toward predicting the array response to transient single events rather than detailed particle interactions within an individual pixel. The model has numerous adjustable parameters. One purpose of the testing was to calibrate the parameters for the REACT model to give the best fit to the observed test data. Testing over a range of energies and angles of incidence provides a means to calibrate the model parameters.

The two primary areas of concern are the distribution of transients across the FPA and their recovery time (or persistence). The distribution of transients (number and spatial distribution) impacts the effective noise level of the IR observations and thus the quality of the science data. The number of pixels affected by transients during an integration period depends on the number of particles that are incident, the spread of charge from the hit pixels to neighboring pixels, and the secondary particles that accompany the primary particle into the detectors. Each particle that hits the array results in a single event that adds noise charge to one or more pixels, creating a cluster of disturbed pixels. The distribution of the single event clusters is key information of interest. Transient recovery time is a concern only if the disturbance persists after reset since there are multiple reset-

read cycles during an integration period. That is, we want to be assured that only one read is affected by each transient event.

## ***Transient Distribution***

The test data provides the spatial distribution of charge deposits in the array for a mono-energetic and mono-directional proton fluence. We have performed extensive data reduction on the proton test data. Initially the datasets were "cleaned" by removing hot pixels and fixed pattern noise. The charge in each pixel was determined as the difference between the first read after reset and the final read for the integration period. The data were then binned into 100 electron bins to form histograms. We have selected to look at four basic types of distributions for comparing the test data to model predictions.

**Pixel charge:** The charge in each pixel is noted and the data set is histogrammed. There are no selection criteria for the pixels. We simply plot what is there, including the pixels that are hit by a proton or a secondary electron, and the pixels that are contaminated by charge leakage from a neighboring hit.

**Peak charge:** The charge in each hit pixel is noted and the data set is histogrammed. In this case the charge that leaks to neighboring pixels by diffusion or secondary particles is not counted. We used a 5 sigma selection criterion to identify which pixels had been hit. Sigma was determined on a row-by-row basis as the standard deviation for each row.

**Total charge:** The total charge deposited by each single event, including the hit pixel and its neighbors, is summed and the data set is histogrammed. The primary proton will produce charge in the hit pixel. Charge will also be deposited in neighboring pixels due to diffusion and due to secondary electrons (deltas) that are generated in the hit pixel but transport to a neighboring pixel and deposit charge.

**Cluster:** The number of pixels that are affected by each hit is histogrammed. First isolated single event hits are identified. Then selection criteria are used (e.g., 5 sigma above the mean) to tag neighboring pixels as being affected by the hit. A histogram is then formed for the number of occurrences for each cluster size.

These four types of distributions were developed from the test data for cases of energy / angle as: 30 MeV / 0 degrees, 30 MeV / 67 degrees, 63 MeV / 0 degrees, 63 MeV / 67 degrees. These four test conditions were simulated with the REACT model using parameters based on input from Rockwell, educated guesses and some trial and error.

Table 1 lists the primary model parameters that were used for the data discussed in the following. Note that we use a slight bias field that nudges carriers toward the junction to simulate the proprietary built-in bias that Rockwell has stated they have due to a grading of the doping through the n-region of the diode. The model data was then used to produce similar single event distributions to what was done for the test data.

**Table 1. Key Model Parameters**

pitch=	18	um
active layer thickness=	8.5	um
depletion width=	0.8	um
diffusion length=	35	um
Ez=	-100	V/cm
Wd=	1.2	eV/e
Rfront=	0	
Rback=	0	
fill factor=	1	

In the simulation, energy deposition along the primary particle path determines the source carriers that are transported through the array to eventual capture or recombination. Our initial modeling assumed a constant LET, but this model produced results that did not agree with the test data in terms of the width of the pulse height distributions. Monte Carlo simulations were performed with the GEANT4 transport code by the Vanderbilt group for proton-induced energy deposition in HgCdTe and the results showed a surprising variance in energy deposition. This variance of LET is primarily due to the large number of discrete secondary electrons along the ion path that transport energy outside the immediate vicinity of the ion track. We simulated this variance in the REACT code for each particle by randomly sampling a Gaussian probability distribution function with a width representative of the GEANT4 results.

Figures 1-4 compare the distributions from the model and from the test data for the 30 MeV case. Similar results were obtained for the 63 MeV, 0 degree case. There is noise in the test data for the 63 MeV, 67 degree data that could not be removed so that data is less reliable.

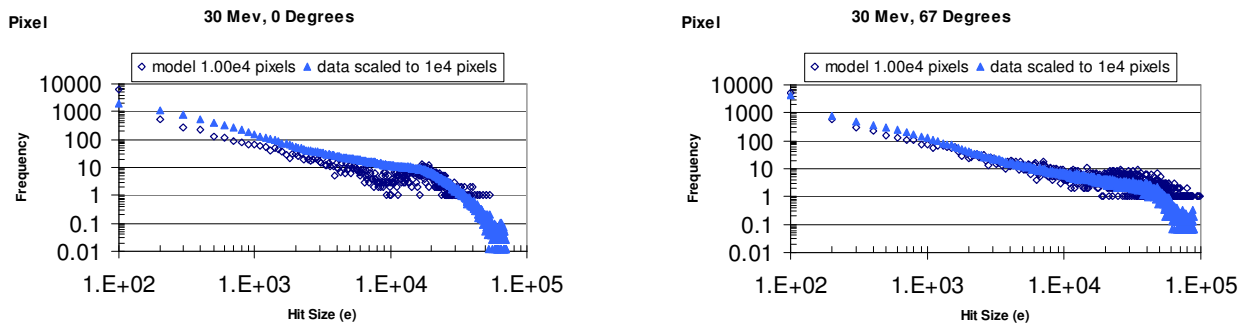


**Figure 1. Distribution of pixel charge transients in detector array due to 30 MeV protons. Model results for 1E4 pixels are compared to test data scaled to 1E4 pixels for 0 degrees and 67 degrees.**

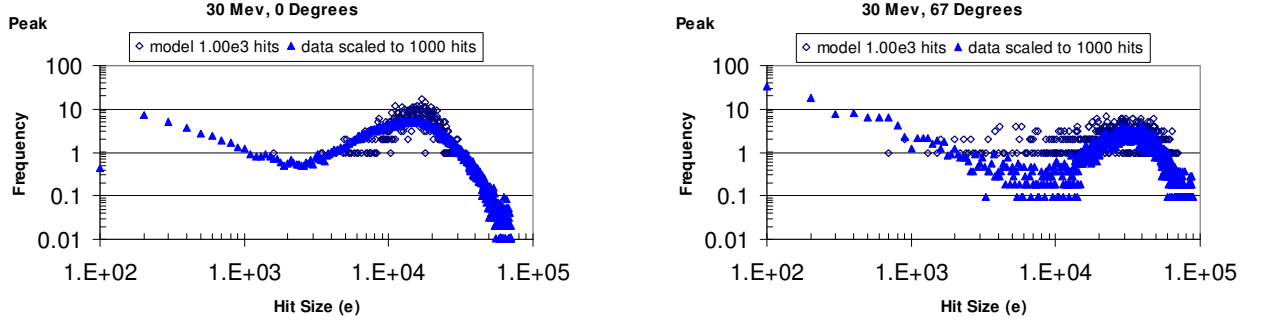


**Figure 2.** Distribution of peak charge transients in detector array due to 30 MeV protons. Model results for 1000 hits are compared to test data scaled to 1000 hits for 0 degrees and 67 degrees.

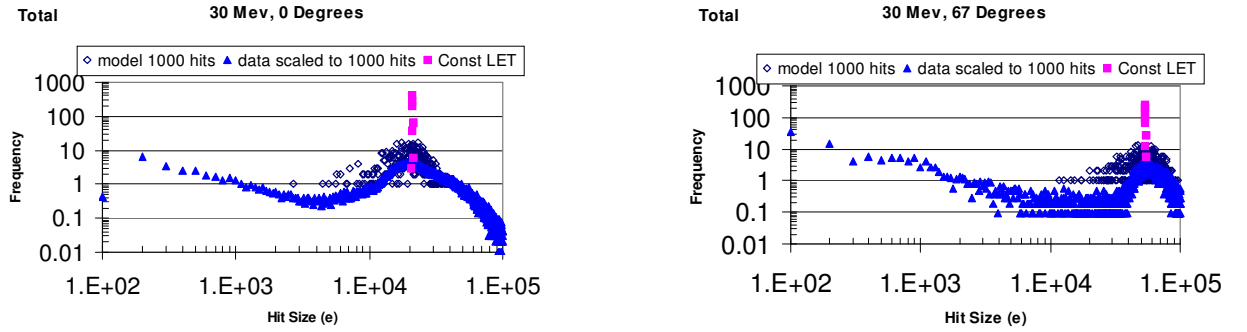


**Figure 3.** Distribution of total charge transients in detector array due to 30 MeV protons. Model results for 1000 hits are compared to test data scaled to 1000 hits for 0 degrees and 67 degrees. The line at the peak is the model result using constant LET. The REACT model prediction with variant LET based on GEANT model for charge deposit distribution agrees well with the data.

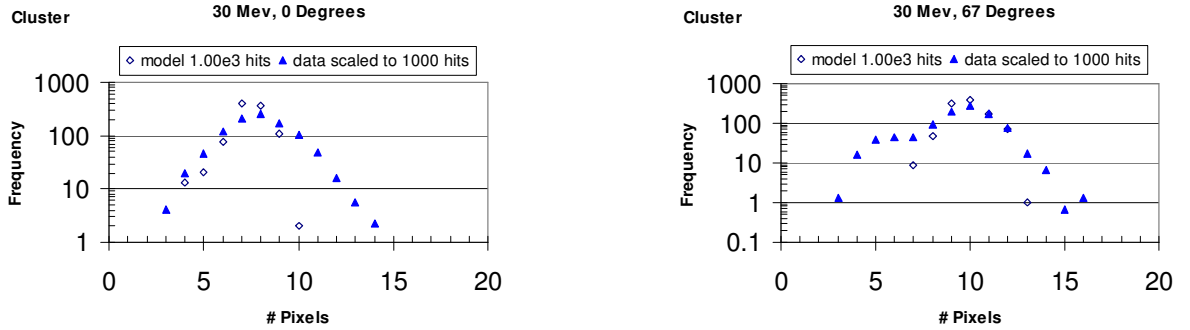


**Figure 4.** Distribution of single event cluster size in detector array. Model results for 1000 hits are compared to test data scaled to 1000 hits for 0 degrees and 67 degrees. The selection criteria was  $>10$  electrons for the model and  $> 5$  sigma ( $\sim 200$  e for 0 degrees,  $\sim 160$  electrons for 67 degrees) for the data.

A quantitative comparison can be made with the weighted averages of the distributions. Table 2 compares the model (M) and data (D) weighted averages for the peak distribution, total distribution and cluster distribution for the four cases. We note fairly good agreement for the location of the peaks of the distributions with this particular set of

model parameters. Note that the cluster data distribution is considered unreliable because of high noise in the raw data.

**Table 2. Comparison of Weighted Averages for REACT Model Distributions and Test Data Distributions**

Run	E	theta	Peak-M	Peak-D	Total-M	Total-D	Cluster-M	Cluster-D
2	30	0	1.65E+04	1.70E+04	2.08E+04	2.20E+04	7.44	7.94
13	30	67	3.09E+04	3.21E+04	5.44E+04	5.24E+04	9.88	9.40
19	63	0	9.69E+03	8.89E+03	1.23E+04	1.30E+04	6.63	6.22
14	63	67	1.81E+04	2.14E+04	3.14E+04	3.27E+04	8.91	5.03

Another validation check is the scaling of the peaks with energy and angle. The average LET of 63 MeV protons is 0.59 times the average LET of 30 MeV protons. The  $\cos(\theta)$  dependence means that 67 degree incidence should deposit 2.56 times the energy deposited at 0 degree incidence. Table 3 compares the energy and angle scaling for the model and the test data. We note the expected scaling with energy for both the model and the data. The scaling with angle is in accordance with  $\cos(\theta)$  for the total charge distributions for both model and data. Note that the peak charge distributions do not follow the  $\cos(\theta)$  dependence as well. This is probably due to the geometry of the pixel, i.e., for the total charge distribution we have a semi-infinite slab geometry where the  $\cos(\theta)$  dependence is expected to hold, but for the peak distribution, we have a rectangular parallelepiped geometry and edge effects may reduce the  $\cos(\theta)$  dependence.

**Table 3. Scaling with Energy and Angle. Results are normalized to 30 MeV and 0 degrees.**

E	LET	Scale Factors				
30	8.43	1				
63	4.95	0.59				
$\theta$						
0		1				
67		2.56				
Energy Scaling						
Run	E	theta	Peak-M	Peak-D	Total-M	Total-D
2	30	0	1.00	1.00	1.00	1.00
13	30	67	1.00	1.00	1.00	1.00
19	63	0	0.59	0.52	0.59	0.59
14	63	67	0.59	0.67	0.58	0.62
Angle Scaling						
Run	E	theta	Peak-M	Peak-D	Total-M	Total-D
2	30	0	1.00	1.00	1.00	1.00
13	30	67	1.88	1.88	2.62	2.38
19	63	0	1.00	1.00	1.00	1.00
14	63	67	1.87	2.41	2.56	2.53

The peak charge and total charge distributions from the model (Figures 2 and 3) more closely follow the data when we use a distribution of LET (based on GEANT modeling) that is centered around the average value determined from SRIM, rather than a constant LET. It seems clear from the data that there is a significant variance on energy

deposition. Simulating this by using a distribution of LET based on the GEANT results seems to give a fair agreement.

For the cluster distributions, the model distribution (Figure 4) is generally not as wide as the data distribution. Note that we used a 10 electron selection criterion for the model distribution while the test data reduction distribution used a 5 sigma ( $\sim 200$  electrons for 0 degrees,  $\sim 160$  electrons for 67 degrees) criterion. The test data results suggest that there may be considerably larger clusters at the 10 electron level that we could not observe in the test data due to the noise levels. We are currently speculating that the difference between the cluster distributions for the model and data may be due to energy transport to pixels near the hit pixel by delta electrons generated along the proton path in the hit pixel. That is, some of the charge leakage to the neighboring pixels is due to diffusion and some may also be due to delta electrons. In the model, we currently only account for diffusion and this may be the reason for the smaller cluster distribution width in the model compared to the data. This issue needs to be further studied.

Analysis of the cluster data from the test results also looked at the effect of the selection criteria and the effect of the primary hit size on the cluster size. Figures 5 and 6 show the effect of the selection criteria on the cluster distributions over the range from 2 to 5 sigma. We see that the distribution widens for lower sigma, as expected. As we lower the selection criteria, the test data reveal some very large clusters, although they are relatively rare.

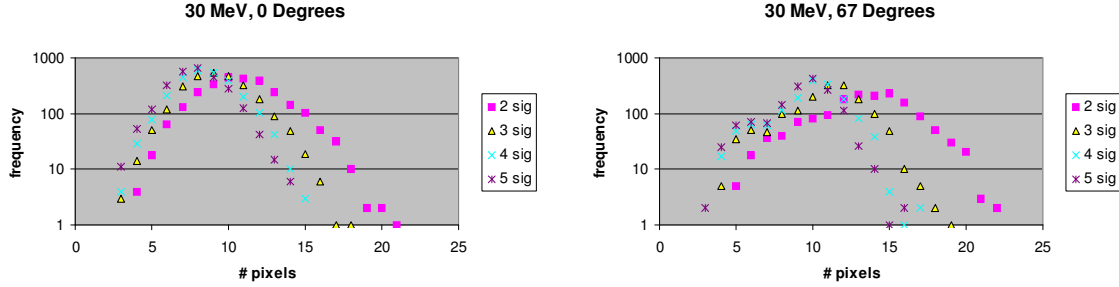


**Figure 5. Effect of Selection Criteria on Cluster Distribution for 30 MeV Data.**

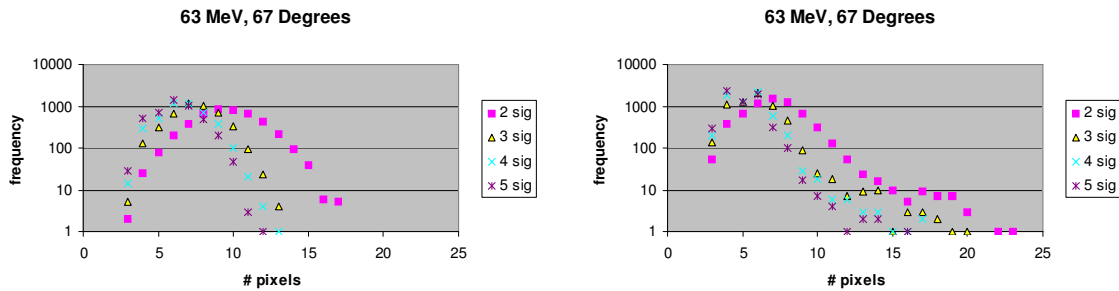


**Figure 6. Effect of Selection Criteria on Cluster Distribution for 63 MeV Data.**

Figure 7 compares the model results to the data for the weighted average of cluster size using various selection criteria. Discounting the 63/67 data, which has high noise, the model seems to be underestimating the cluster size. The reason for this may be the fact that the current model does not account for energy transport to neighboring pixels by delta electrons.

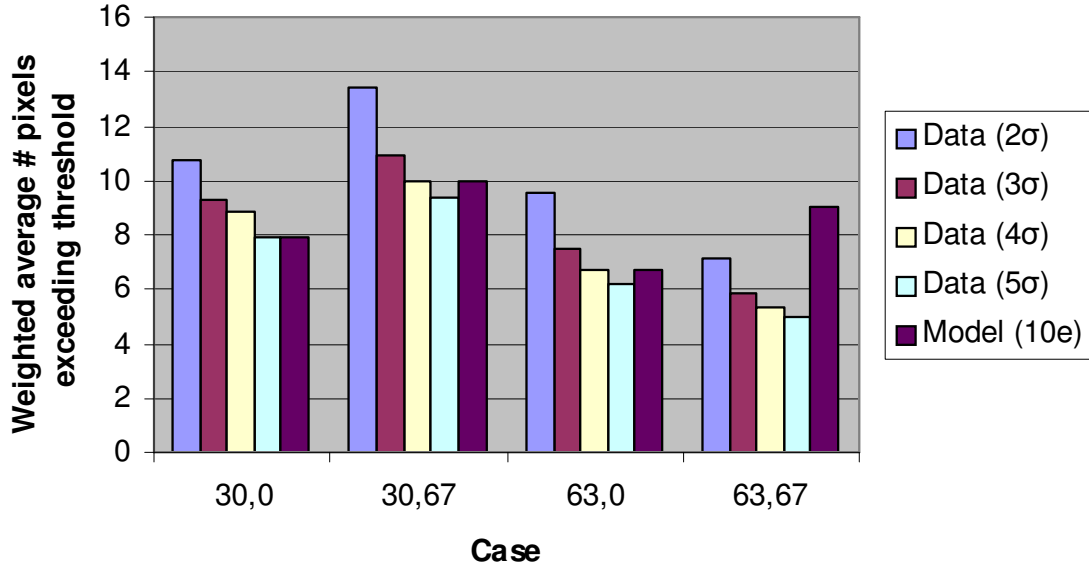


Figure 7. Weighted average cluster size for various selection criteria compared to model.

Figure 8 shows the effect of the pulse size on the cluster distribution for 30 MeV data. Similar trends were seen for the 63 MeV data. The data were binned into 20,000 electron bins based on the size of the transient. We note that the clusters scale with pulse size, i.e., bigger pulses produce bigger clusters, as seems logical. This is good news for the mission since the pulses from the GeV protons are somewhat smaller than the pulses from the test data. For example, the average LET of a 1GeV proton is 0.94 keV/ $\mu$ m compared to 6.85 keV/ $\mu$ m for a 30 MeV proton. However, this effect needs further study in order to quantify.

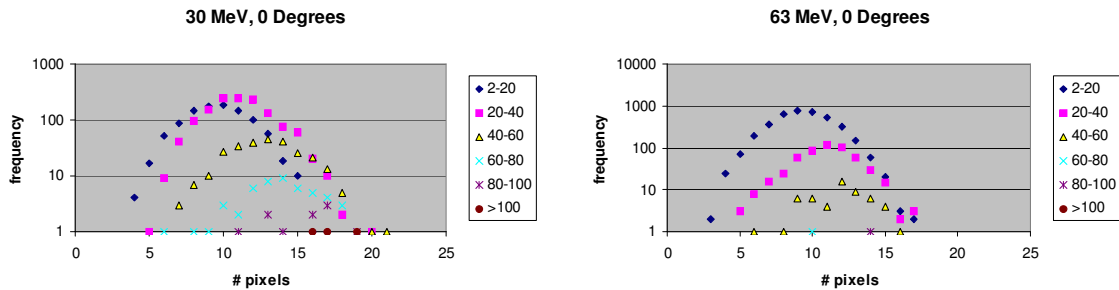
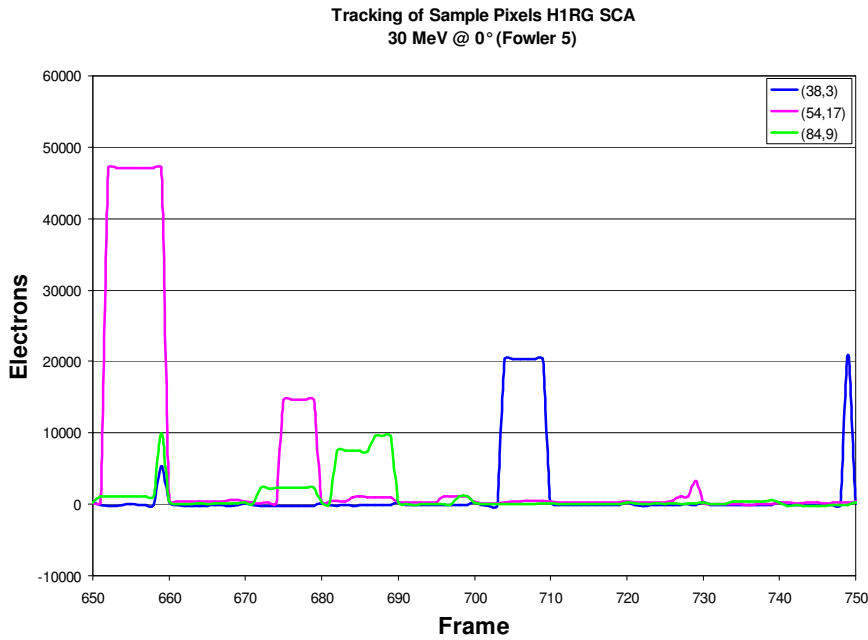


Figure 8. Effect of pulse size on cluster distribution.

## Recovery Time

Figure 9 shows pixel response to 30 MeV protons, with a Fowler-5 read mode (100 ms read cycle with reset after every 10th frame). The charge in three pixels is shown across several frames. In many cases there are proton hits during the frames. The reset at the end of every tenth frame removes any evidence of the charge in the hit pixel down to the noise levels during testing, which was a one sigma value of  $\sim 40$  electrons. From the test data, we cannot say for certain that charge transients down to the JWST level of 10 electrons have been cleared. However, this data does demonstrate that there is no long term recovery that completely overwhelms that pixel.



**Figure 9. Pixel charge recovery after proton hits. Data are shown for 3 pixels across several frames.**

The data shows that the transient charge deposition to the pixel is faster than 100 ms. This can be seen because the charge in the pixel is flat after a hit until reset. For example, in the figure we note that there is a reset at frame 680 and again at frame 690. There is a hit at about frame 685 and the pixel charge jumps up and stays constant until reset at frame 690. Since there is 100 ms between reads and the charge does not change after the hit frame, it can be concluded that the transient for the charge deposition is faster than 100 ms. Since the transient recovery time is faster than any integration or reset time of interest to JWST, we conclude that transient recovery time is not an issue at the  $\sim 40$  electron noise level applicable to these data. However, it remains to be shown conclusively that persistence through reset down to the 10 electron level is not a problem.

## Summary

- An extensive series of tests were performed on prototype JWST FPAs at a cyclotron using 30 and 63 MeV protons and varying angle of incidence.
- An engineering model of energetic particle interaction with the FPA was developed to predict the spatial distribution of charge deposits during an integration period due to energetic particles impacting the FPA. The model does not address temporal effects.
- Using geometry and device information from Rockwell, along with educated guesses and trial and error, the REACT model was compared to the test data and model parameters were calibrated to give a best fit between model and data. Calculations with GEANT for proton energy deposits in HgCdTe samples representative of the pixel geometry predict significant variance in proton energy deposition. That is, there is a variance in effective LET. Getting agreement between the model and data distribution widths for total charge required assumption of a LET variance similar to the GEANT calculations.
- The REACT model successfully predicts the overall characteristics of the pulse height distributions observed during the testing and exhibits expected scaling with energy and angle of incidence.
- The model predicts the average values of cluster sizes at the 5 sigma charge levels, ~200 electrons, which was the noise limit at the cyclotron. Analysis of the test data at lower sigma thresholds suggests that there are significantly larger clusters in the test data than can be explained by the model using only diffusion as a lateral transport mechanism. The model under predicts the cluster distribution widths, i.e., there are larger clusters in the test data than predicted by the model.

## Unresolved Transient Modeling Issues

- Role of delta electrons generated along ion track within pixel in lateral energy transport to nearby pixels and the impact on cluster size at the 10 electron level.
- Role of delta electrons in material external to pixel causing hits in nearby pixels to the primary hit pixel. We also need to pay attention to the massive In column that is in intimate contact with the sensitive region of all pixels.
- Methodology to quantify cluster distribution at GeV range GCR protons based on measurements with lower energy accelerator protons, i.e., scaling with LET.
- Methodology to quantify cluster distribution at 10 electron level. Current cyclotron measurements have a noise level that is at least a factor of 4 or more higher than the flight noise level of 10 electrons. Current modeling predicts

cluster distributions that are smaller in width than observations from test data distributions.

- Determination if there is post-proton persistence through reset down to the 10 electron level.

### Recommendations

- Continue with detailed delta electron studies using GEANT and NOVICE to quantify charge transport by deltas to pixels nearby the hit pixel. Consider delta production both within the pixel and within material surrounding the pixel. Integrate the delta results with REACT.
- Perform transient measurements at the 10 electron level. This will likely require an Ultra-Low Background dewar and ultra-low noise measurements at the proper facility.